

Available online at [www.sciencedirect.com](http://www.sciencedirect.com)**ScienceDirect**

Energy Procedia 63 (2014) 4411 – 4417

Energy

**Procedia**

GHGT-12

## Microseismic Monitoring at the Large-Scale CO<sub>2</sub> Injection Site, Cranfield, MS, U.S.A.

Makiko Takagishi<sup>a\*</sup>, Tsutomu Hashimoto<sup>a</sup>, Shigeo Horikawa<sup>b</sup>, Kinichiro Kusunose<sup>c</sup>,  
Ziqiu Xue<sup>a</sup>, Susan D Hovorka<sup>d</sup>

<sup>a</sup>Research Institute of Innovative Technology for the Earth (RITE), 9-2 Kizugawadai, Kizugawa-shi, Kyoto, 619-0292, Japan

<sup>b</sup>Suncoch Consultants Co., Ltd., 1-8-9 Kameido, Koto-ku, Tokyo, 136-8522, Japan

<sup>c</sup>The National Institute of Advanced Industrial Science and Technology (AIST), 1-1-1, Higashi, Tsukuba-shi, Ibaraki, 305-8567 Japan

<sup>d</sup>Bureau of Economic Geology, Jackson School of Geosciences, The University of Texas at Austin, Austin, Texas, U.S.A.

---

### Abstract

This paper describes passive seismic monitoring at the large-scale CO<sub>2</sub> injection site, Cranfield oilfield, Mississippi, U.S.A. We constructed a horizontal near-surface monitoring network and have been monitoring for more than two years to elucidate relationship between large-volume CO<sub>2</sub> injection and occurrences of induced seismicities. We have detected no microseismic events that occurred in and around the Cranfield site for now. The detected signals were all identified as cultural noises, natural noises due to weather changes, and distant earthquakes. We also estimated minimum detectable magnitudes of the monitoring network by theoretical calculations and confirmed that the system could enough ability to detect microseismic events.

© 2014 The Authors. Published by Elsevier Ltd. This is an open access article under the CC BY-NC-ND license

(<http://creativecommons.org/licenses/by-nc-nd/3.0/>).

Peer-review under responsibility of the Organizing Committee of GHGT-12

**Keywords:** Geological Storage; Induced seismicity; Microseismic monitoring; Cranfield

---

---

\* Corresponding author. Tel.: +81-774-75-2312; fax: +81-774-75-2316.

E-mail address: [takagishi@rite.or.jp](mailto:takagishi@rite.or.jp)

## 1. Introduction

Increase number of injection induced seismicity has been raised public concern in the recent years. These felt earthquakes with usually magnitudes  $M > 3$  are induced by fluid injection associated with oil and gas production and reported in the central and eastern United States, where regional seismicity is not active [1].

Carbon dioxide capture and storage (CCS) is a key potential technology for reducing greenhouse gas emission. Supercritical state  $\text{CO}_2$  is injected to porous sandstone or dolomite reservoir. Due to long-term and large-amount of injection under high pressure, it is controversial that CCS might trigger felt earthquakes like other fluid injection activity [2], [3]. Therefore, assurance of safe operation against injection induced seismicity is one of the most critical issues for CCS operators.

Passive microseismic monitoring is a direct measurement technique to observe geological responses, and the technique, mainly developed from the oil and gas production industries, has been applied at CCS sites to ensure the storage security. Reported microseismic events clearly related to  $\text{CO}_2$  injection were all unfelt [3], and most of the events were with negative magnitudes [4]. Even though  $\text{CO}_2$  injection induces only small magnitude of unfelt events, importance of passive microseismic monitoring at the injection site is being recognized.

Cranfield oilfield, located in the southeast part of the United States, is a large scale  $\text{CO}_2$  - enhanced oil recovery (EOR) site, where more than one million metric tonnes of  $\text{CO}_2$  is annually stored at the sandstone reservoir. At the site, we constructed a near-surface monitoring network and conducted microseismic monitoring to elucidate relationship between large scale  $\text{CO}_2$  injection and induced microseismicity. In this study, two years of microseismic monitoring at Cranfield is reported.

## 2. Cranfield oilfield

We selected Cranfield oilfield as a monitoring field. For site selection, it was important to select a site where large volumes of  $\text{CO}_2$  are being injected, where abundant data about the reservoir and overburden are available, and where the site operator was willing to host. The Cranfield oilfield met all of these requirements. The Cranfield oilfield is located in a rural area of southwestern Mississippi near the Louisiana border shown with the red circle symbol (Fig. 1a). Natural  $\text{CO}_2$  is supplied from Jackson dome which is about 100km northeast of the site, and transferred by pipeline.  $\text{CO}_2$  -EOR floods started in 2008, and more than four million metric tonnes of  $\text{CO}_2$  have been stored as of the beginning of 2013 [5]. The oilfield holds an area of about with 3 km radius. The field development area is spreading in a clockwise from north part of the field around (1) 44-6 station (Fig. 1(b)), and the number of  $\text{CO}_2$  injection and production wells is also increasing. The development front reached south part of the field around (6)68-3 station as of January, 2014 holding about 30  $\text{CO}_2$  active injection wells and about 30 active production wells.

Injection zone is the lower Tuscaloosa formation in a broad four-way structural closure at a depth greater than 3,000m with porosity and permeability of 20 ~ 30% and 10 ~ 200 mD, respectively. Dark marine mudstone overlying the injection zone performs as a confining layer [6]. Regional natural seismicity is quite low. If any suspicious seismic events are recorded, signals will be easily distinguished from those of natural earthquakes.

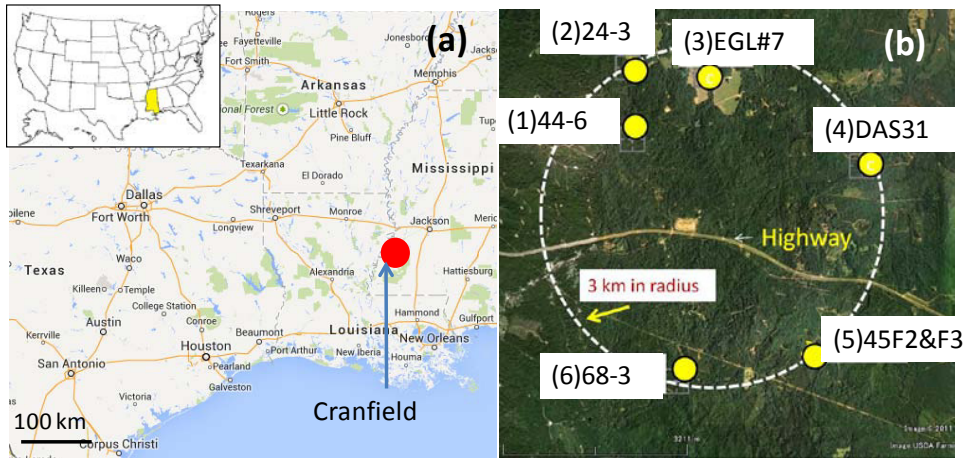


Fig. 1. (a) Location of the Cranfield site; (b) Map of the monitoring network. Six near-surface stations were deployed in a 3km radius area to cover the entire area of the Cranfield site.

### 3. Passive microseismic monitoring

We constructed a near-surface microseismic monitoring network which consists of six seismometers deployed in a 3km radius to cover the entire area of the field (Fig. 1(b)). Three components of 1Hz servo-type velocity seismometers with the frequency range of 0.018 ~ 80Hz were installed at the depth of 90 m to suppress the noises. This type of servo-type velocity seismometers can measure small to large seismic events because of the wide frequency and wide amplitude range. In Japan, this type of the sensor is used for earthquake observation network such as F-net in Japan [8]. Signals are measured continuously up to 5 cm/s with 24 bit A/D resolution at the sampling frequency of 200 Hz. We started microseismic monitoring on December 15, 2011 and it has been monitored more than two years as of January, 2014.

The average noise levels for all three components range from  $10^{-4}$  to  $2 \times 10^{-4}$  cm/s at each site. The frequency characteristic has two apparent peaks. The lower peak ranging from 0.1 to 0.2 Hz is the microseisms, and the higher ranging from 5 to 6 Hz is due to the characteristic beneath the site. Microseismic events supposed to have higher frequencies; therefore we decided to apply Butterworth highpass filter at the cutoff frequency of 2Hz to eliminate the microseisms. The average noise levels decreased to 10% ranging from  $10^{-5}$  to  $2.0 \times 10^{-5}$  cm/s compared to those of original waveforms.

### 4. Data processing

#### 4.1. Extraction of candidate microseismic events

Signal processing was performed to extract microseismic events. We assumed that microseismic events related to CO<sub>2</sub> injection had similar appearances and properties to natural tectonic earthquakes. Therefore, we put following three criteria to extract microseismic events. First, the signals are detected at several stations if the microseismic events occur at the site. Second, P-wave arrival times are almost the same at each station. Arrival time differences are at most two seconds based on geometry of the site. Third, microseismic events have clear P- and S- wave arrivals. Then, vertical components of data were examined to extract candidate microseismic signals by semi-automated method. If the absolute values of velocity amplitude exceed threshold determined by more than 10 times of average noise levels almost at the same time at four or more than four out of six stations, we regarded signals were triggered. After that, natural distant earthquakes and noises due to the weather changes were eliminated from the candidate signals manually by referring the earthquake catalogues opened by U.S. Geological Survey (USGS) and weather data opened by Weather Underground. Then the candidate signals were examined if the signals had

both clear P- and S-wave arrivals.

At the beginning of the data processing, we also decided to examine data by visual judgments until sufficient number of microseismic events related to CO<sub>2</sub> injection was detected. The initial semi-automated processing method was going to be modified based on characteristics of detected microseismic events. Candidate microseismic events were extracted using filtered Z-components of data. If the velocity amplitudes are apparent at four or more than four stations almost at the same time, we regarded the signals were triggered. Then earthquakes and noises due to weather changes are eliminated in the same manner as the signal processing. The reminded candidate signals were checked if the clear P- and S- wave arrivals were seen using three components of the data.

#### 4.2. Results

As a result of data processing, no microseismic events were detected at the Cranfield site from two years of monitoring data. The triggered signals were all identified as background noises, cultural noises such as constructions, and noises due to the weather changes such as precipitation, lighting strikes, strong winds, and a total of 253 natural distant earthquakes ( $M_w$  2.5 to 8.6) that occurred at least more than 300 km away from the Cranfield site. Fig. 2 indicates three components of waveforms that occurred in Eastern Texas on May 10<sup>th</sup>, 2012 with  $M_w$  3.9 at the distance of about 300 km. Clear P- and S-wave arrivals are recognized at around 90s for Z-component and 120s for X and Y components, respectively.

Fig. 3 indicates Z-components of waveforms at each station (the data at 24-station was not available due to the technical problem). Recorded signals are identified as noises due to the lighting strikes that occurred around the site. Even though the peaks are seen at each station, arrival times and velocity amplitudes are different. For the noises due to weather changes, peaks are recognized frequently in a short period of time.

We examined all the recorded data by visual judgments consequently, and we did not find any microseismic events, either. This result is in a good agreement with the semi-automated data processing.

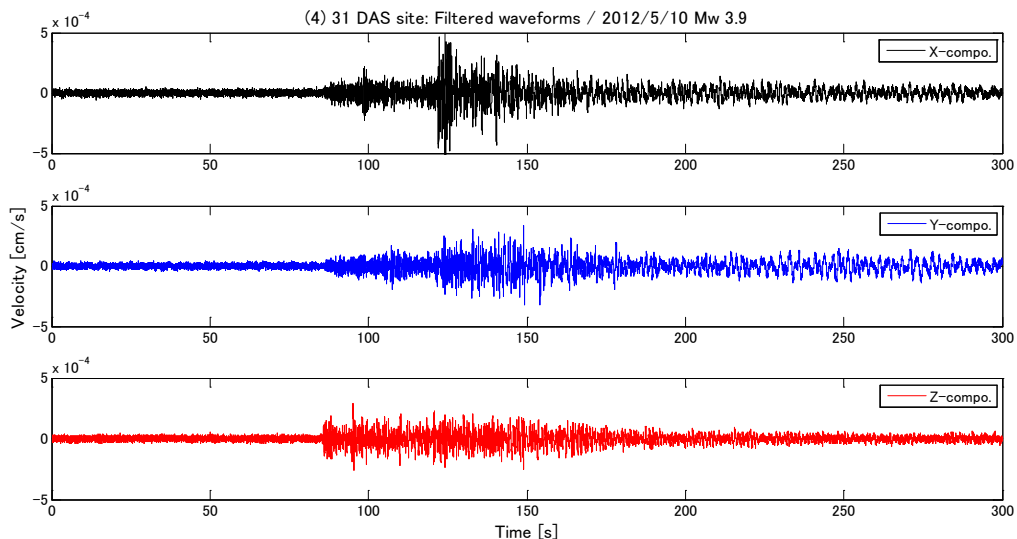


Fig. 2 Three components of waveforms that occurred at Eastern Texas with magnitude of  $M_w$  3.9 at the Epicentral distance of about 300 km on May 10, 2012.

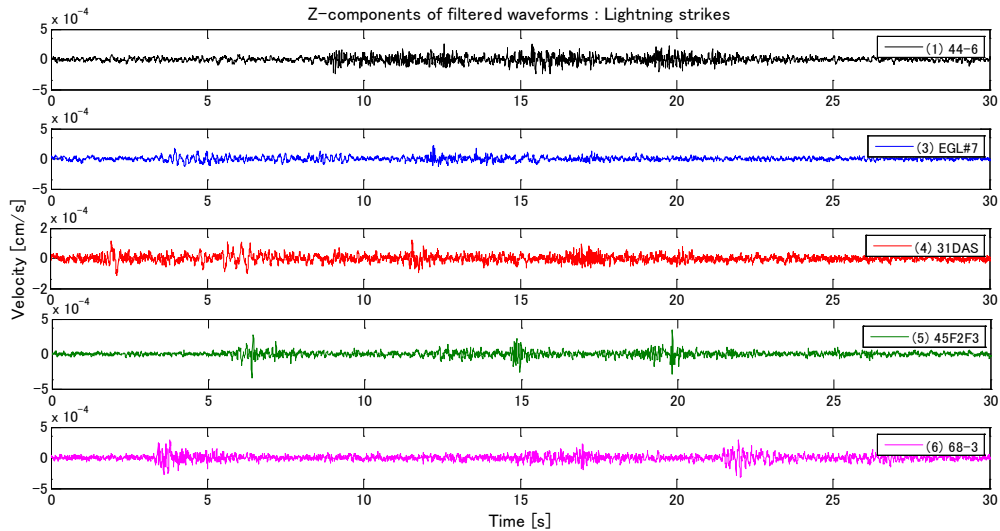


Fig 3 Z-component of waveforms recorded at five stations. These peak amplitudes are noises due to lightning strikes.

Fig. 4 indicates the magnitude and distance relation of natural earthquakes that occurred within 1,000 km at the Cranfield site. Grey circle symbols are a total of 2079 earthquakes reported by USGS, and the red diamond symbols are 15 detected earthquakes by the Cranfield monitoring network. The estimated limits of detectable magnitude and distance are shown in blue solid lines. Two lines indicate the possible detection limits. During the day time, the noise levels get higher due to cultural noises, the detectable limits move to the right side, whereas during the night-time, the detectable limits move to the left side.

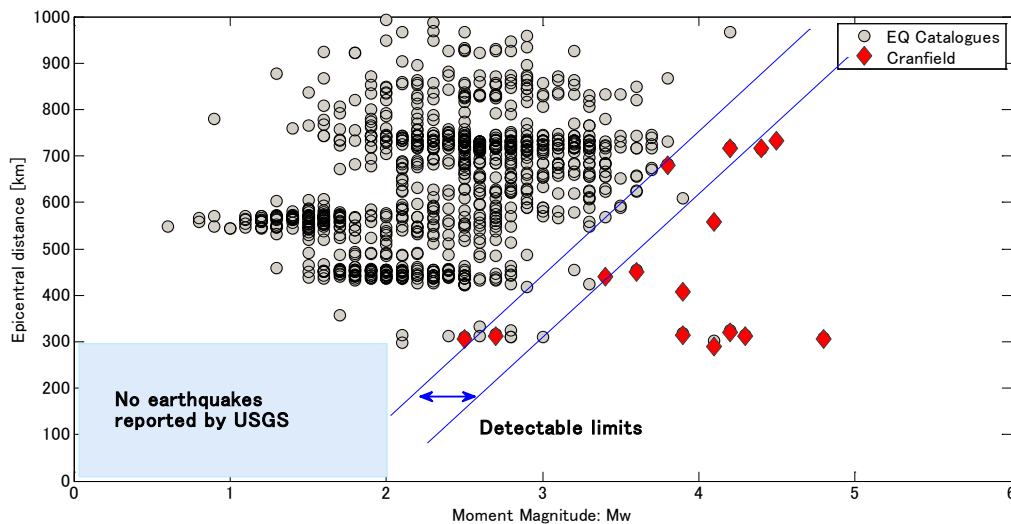


Fig. 4 Relation of moment magnitudes  $M_w$  and Epicentral distances from the Cranfield site [km]. Grey circle symbols ( $n=2079$ ) are the natural earthquakes reported by USGS, and red diamond symbols are recorded earthquakes ( $n=15$ ) at the Cranfield site. Blue solid lines indicate the detectable limits of magnitudes and Epicentral distances.

## 5. Estimation of detectable minimum magnitudes at the Cranfield

To obtain the detectability of the monitoring network, we estimated minimum detectable magnitudes of our microseismic monitoring system by waveform synthesis calculations based on discrete wavenumber integration method [9], [10]. Maximum velocity amplitudes of synthesized waveforms at given magnitudes were compared to average noise levels at the site. Waveforms were synthesized with source and transfer properties considering one dimensional geological property model that includes attenuation factors  $Q_p$  and  $Q_s$ , density, P- and S-wave velocities beneath the site. This model was constructed based on logging data obtained at the site. The rupture fault was assumed as a point source because of the small magnitudes. The fault mechanism was assumed as normal fault considering the stress field around Cranfield site. The average noise level was settled on  $20 \times 10^{-5}$  cm/s, equivalent to the upper limit of noise levels for the filtered waveforms.

As the result of the calculation, the minimum detectable magnitudes were estimated for the horizontal and vertical components,  $M_w$  0.4 and 0.7, respectively at the hypocentral distance of 3.2 km (Fig. 5). For the horizontal components, root mean square values of max velocity amplitudes were used.

The upper frequency range of 80 Hz corresponds to between  $M_w$  0 and  $M_w$  1 concerning the scaling law between corner frequency and moment magnitude  $M_w$  [10]. The hypocentral distance and magnitude relation [11] also indicates that around  $M_w$  0 would be the minimum detectable magnitude at the hypocentral distance of about 3km. Therefore, it seems that the obtained results give reasonable value for the minimum detectable magnitudes.

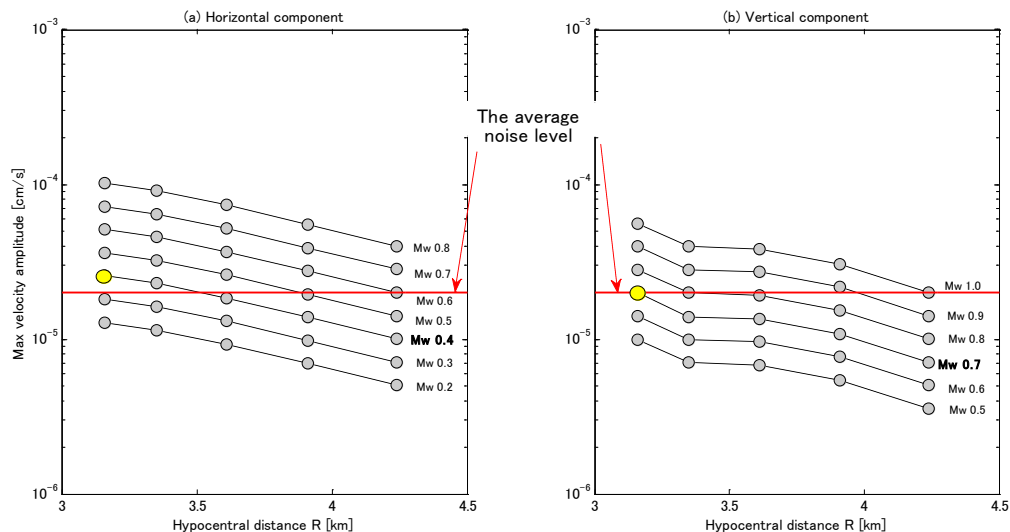


Fig.5 Results of theoretical calculations to estimate minimum detectable magnitudes. (a) Horizontal component (b) Vertical component. The estimated minimum detectable magnitudes are  $M_w$  0.4 and 0.7 for horizontal and vertical components, respectively.

## 6. Conclusions

In this paper, we presented microseismic monitoring at the large scale  $CO_2$  injection site, Cranfield oilfield, Mississippi, U.S.A. We constructed a near-surface microseismic monitoring network and have been monitoring to elucidate the relationship between large scale  $CO_2$  injection and occurrences of induced seismic events. For the first two years of monitoring, we have obtained following two points.

- We detected no seismic events at the Cranfield site through the entire period of two years. Detected signals were identified as background noises, cultural noises, noises due to weather changes, and natural distant earthquakes. The smallest distant earthquake was magnitude  $M_w$  2.5 with the Epicentral distance of 300km.

- Theoretical study showed that the estimated minimum detectable magnitudes were  $M_w$  0.4 for horizontal and 0.7 for vertical components at the horizontal distance of 1km (hypocentral distance of 3.2 km).

We did not detect any seismic events induced by CO<sub>2</sub> injection in and around the Cranfield site for two years, where more than one million tonnes of CO<sub>2</sub> is annually injected. It seems that the stress at the injection zone did not build up enough to trigger microseismic events because of high porosity and high permeability. Seismic monitoring at the Cranfield site will be conducted until December, 2014. At the end of the monitoring, re-analysis of all the data will be performed concerning knowledge obtained during the entire monitoring period.

## Acknowledgements

This work was funded by the Ministry of Economy, Trade and Industry (METI), Japan under the contract research of “Development of Safety Assessment Technology for Carbon Dioxide Capture and Storage”. We would like to appreciate Denbury Onshore, LLC for their contributions Tom Daley and John Beyer at the Lawrence Berkeley National Laboratory for their collaborations. The earthquake catalogue opened by U.S. Geological Survey (<http://earthquake.usgs.gov/earthquakes/search/>) and weather data opened by Weather underground (<http://www.wunderground.com/>) were used.

## References

- [1] Ellsworth WL. Injection-induced earthquakes, *Science*. 2013; 341, 1225942.
- [2] Zoback MD, Gorelick SM. Earthquake triggering and large-scale geologic storage of carbon dioxide. *Proc. Natl. Acad. Sci.* 2012; 109(26), 10164 -10168.
- [3] National Research Council. *Induced Seismicity Potential in Energy Technologies*, Washington DC: The National Academies Press; 2013.
- [4] Verdon JP, Kendall JM, Stork AL, Chadwick RA, White DJ, Bissell RC. Comparison of geomechanical deformation induced by megatonne-scale CO<sub>2</sub> storage at Sleipner, Weyburn, and In Salah. *Proc. Natl. Acad. Sci.* 2013; 110 (30), 2762-2771.
- [5] Hovorka SD, Meckel TA, Trevino RH. Monitoring a large-volume injection at Cranfield, Mississippi—Project design and recommendations. *Int. J. Greenh. Gas Con.*, 2013; 18, 345-360.
- [6] Lu J, Kordi M, Hovorka SD, Meckel TA, Christopher CA. Reservoir characterization and complications for trapping mechanisms at Cranfield CO<sub>2</sub> injection site, *Int. J. Greenh. Gas Con.* 2012; 18, 361-374.
- [7] Verdon JP, White DJ, Angus DA, Fisher QJ, Urbancis T. Passive seismic monitoring of carbon dioxide storage at Weyburn. *The Leading Edge*, 2010; 29(2), 200-206.
- [7] Okada Y, Kasahara K, Hori S, Obara K, Sekiguchi S, Fujiwara H, Yamamoto A. Recent progress of seismic observation networks in Japan Hi-net, F-net, Kpnet and KiK-net. *EPS*, 2004; 56, p.xv-xxviii.
- [8] Coutant, O. *Programme de Simulation Numérique AXITRA, Rapport LGIT*, Université Joseph Fourier, Grenoble, France; 1990.
- [9] Bouchon M, Aki K. Discrete wavenumber representation of seismic sources wave fields, *Bull. Seism. Soc. Am.*, 1977; 67, 259-227.
- [10] Iio Y. Sscaling relation between earthquake size and duration of faulting for shallow earthquakes in seismic moment between 1010 and 1025 dyne/cm. *J. Phys. Earth*, 1986p 34, 127-169.
- [11] Warpinski NR, Du J, Zimmer U, Measurements of Hydraulic-Fracture-Induced Seismicity in Gas Shale. *SPE* 151597, 2012;